INTERNATIONAL JOURNAL OF PHARMACEUTICAL SCIENCES
[ISSN: 0975-4725; CODEN(USA): IJPS00]
Journal Homepage: https://www.ijpsjournal.com

OPEN ACCESS

Research Paper

Telmisartan - nanocrystal innovative approach to enhance oral bioavailability

Dr. Nimita Manocha*, Garima Bairagi, Nayany Sharma, Dr. Nadeem Farooqui

Indore Institute of Pharmacy, Indore, (M.P.), India .

ARTICLE INFO

Published: 18 May 2026
Keywords:
Telmisartan, nanocrystals, oral bioavailability, poorly soluble drug, nanotechnology
DOI:
10.5281/zenodo.20268436

ABSTRACT

Telmisartan is a BCS class II antihypertensive medication that has low oral bioavailability due to its poor aqueous solubility and slow rate of dissolution. The goal of the current study was to create nanocrystal formulations that would enhance telmisartan's dissolution behaviour. To create an ideal formulation, nine batches of telmisartan nanocrystals were made and assessed. To evaluate size distribution and physical stability, the prepared nanocrystals were measured for particle size, polydispersity index, and zeta potential. To assess drug incorporation within the nanocrystal system, drug content and entrapment efficiency were calculated.In order to evaluate size reduction, uniformity, and physical stability, the prepared Scanning electron microscopy was used to analyze the nanocrystals' surface morphology. Fourier-transform infrared spectroscopy was used to investigate drug-excipient compatibility. The outcomes verified the successful formation of stable, nanoscale telmisartan crystals. When compared to the pure drug, the optimized nanocrystal formulation exhibited better dissolution behaviour. Overall, the study shows that nanocrystal formulation is a useful strategy for improving telmisartan's dissolution performance.

INTRODUCTION

The aqueous solubility of medications is one of the most difficult problems in the field of pharmaceutical sciences [1]. The fact that a significant percentage of both approved medications and newly developed active candidates have poor water solubility makes this problem worse [2]. Currently, about 70% of pharmaceutical agents being studied are classified as Biopharmaceutics Classification System (BCS) class II, which has dissolution rates that limit absorption due to reduced solubility. A lower rate of dissolution that compromises bioavailability and biodistribution is referred to as "low solubility" [3]. The achievement of an ideal therapeutic concentration is hampered by this

***Corresponding Author:** Dr. Nimita Manocha
Address: *Indore Institute of Pharmacy, Indore, (M.P.), India ..*
Email ✉: nimita.manocha@indoreinstitute.com

Relevant conflicts of interest/financial disclosures: The authors declare that the research was conducted in the absence of any commercial or financial relationships that could be construed as a potential conflict of interest.

decreased dissolution rate, highlighting the crucial significance of resolving solubility issues in pharmaceutical formulations [1,4].Because of an increased surface area to volume ratio and better dissolution rates (i.e., dissolution velocity) linked to nanosizing, nanocrystalline drug technology increases the solubility of hydrophobic drugs.8 For the rehabilitation of previously unsuccessful Biopharmaceutics Classification System (BCS) Class II and IV drugs (low solubility drugs), the drug crystals are exceptionally well suited.9 The BCS classification system is an experimental model that assesses solubility and permeability under specific circumstances. The drugs are categorized into four classes by the system. Class I drugs have high permeability and solubility, Class II molecules have high permeability and low solubility, Class III drugs have low permeability and high solubility, and Class IV drugs have low permeability and low solubility.4

MATERIAL

Telmisartan was obtained as a gift sample from Andhra Organics Limited Hyderabad, Telangana, India, Chloroform Ethanol, Dichloromethane, Hydroxypropyl Methylcellulose (E15 grade) HPMC E15, Poloxamer 188, Polyvinylpyrrolidone K15 (PVP K15) Polyvinylpyrrolidone K30 (PVP K30)

Pre-Formulation Studies

Pre-formulation studies were conducted to evaluate the physicochemical properties of Telmisartan and to assess its compatibility with selected excipients prior to formulation development. These studies are essential for understanding the drug's behaviour and for selecting appropriate formulation strategies to enhance its performance.

Organoleptic Properties

The organoleptic properties of telmisartan active pharmaceutical ingredient (API) were evaluated as a part of preformulation studies. The drug was examined visually to assess its colour, odour, and physical appearance.

Solubility Studies

The solubility of Telmisartan was determined in various solvents, including distilled water, methanol, Ethanol, Dichloromethane. An excess quantity of the drug was added to each solvent and agitated continuously for 24 hours at room temperature to attain equilibrium. The resulting solutions were filtered, suitably diluted, and analyzed for drug content using a UV–visible spectrophotometer. These solubility studies were carried out to identify suitable solvents and dissolution media for formulation development and in-vitro evaluation.

Determination of Maximum Absorption Wavelength (λmax)

A standard stock solution of Telmisartan was prepared using methanol as the solvent. The solution was scanned over the wavelength range of 200–400 nm using a UV–visible spectrophotometer to determine the wavelength of maximum absorbance (λmax). The identified λmax was subsequently employed for all further quantitative analytical estimations.

Preparation of Calibration Curve for Telmisartan

From the standard stock solution, a series of working standard solutions of Telmisartan were prepared using Dichloromethane as the diluent. The absorbance of each solution was measured at the predetermined λmax using a UV–visible spectrophotometer. A calibration curve was constructed by plotting absorbance against concentration to assess linearity and to facilitate

accurate quantitative determination of Telmisartan in formulation and in-vitro studies.

Drug–Excipient Compatibility Studies

The compatibility between Telmisartan and the selected excipients—PVP K30, HPMC E15, PVP K15, Poloxamer 188, and Tween 80—was evaluated using Fourier Transform Infrared (FTIR) spectroscopy. FTIR spectra of pure Telmisartan and its physical mixtures with individual excipients were recorded and analyzed. The spectra were compared to identify any significant shifts, disappearance, or formation of new characteristic peaks, which would indicate potential chemical interactions. The absence of such changes confirmed the compatibility of Telmisartan with the selected excipients.

Optimization of Telmisartan Nanocrystals using Design of Experiments (DoE)

A systematic Design of Experiments (DoE) approach was employed to optimise the formulation of telmisartan nanocrystals. The concentrations of PVP K30 (X_1) and HPMC E15 (X_2) were selected as independent formulation variables, as these stabilising agents were anticipated to significantly influence the physicochemical properties and performance of the nanocrystal formulation. A factorial experimental design was adopted, wherein the selected variables were evaluated at different concentration levels.

Table 1 Factors and levels for the optimization of nanocrystals

S.no.	Name of factors	Level	
		low	High
1	Polyvinylpyrrolidone K15 (X1)	2	4
2	Hydroxypropyl methylcellulose(X2)	2	4

The dependent responses chosen for optimisation included drug entrapment efficienc (Y_1) and drug content (Y_2) Zeta potential (Y3). The experimental data obtained from the designed batches were statistically analysed using appropriate software to generate polynomial equations and response surface plots, enabling evaluation of the individual and interactive effects of the formulation variables on the selected responses

Table 2 Response variables with units

S.no.	Response Variable	Unit
1	Percent drug entrapment (Y1)	%
2	Drug content (Y2)	%
3	Zeta potential (Y3)	mv

Select	Std	Run	Factor 1 A:PVP K15 mg	Factor 2 B:HPMC mg	Response 1 Drug entrpm... %	Response 2 Drug Content %	Response 3 Zeta Potential mV
	6	1	4.00	3.00	92.85	92.14	24.6
	4	2	4.00	4.00	93.72	93.25	28.3
	8	3	3.00	4.00	94.18	94.86	31.5
	3	4	2.00	4.00	95.02	95.12	35.2
	5	5	2.00	3.00	95.67	96.04	41.8
	1	6	2.00	2.00	96.24	96.78	52.4
	9	7	3.00	3.00	97.58	97.45	69.3
	2	8	4.00	2.00	91.92	95.89	33.1
	7	9	3.00	2.00	96.86	94.73	46.7

Figure 1 Effect of formulation variable on drug entrapment efficiency and drug content of Telmisartan nanocrystal

a. Effect of X1 and X2 on Y1 The effect of X1 and X2 on Y1 is shown by Figure.

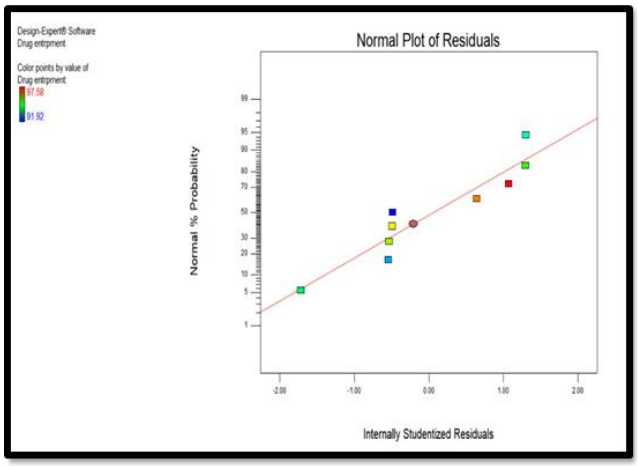

Figure 2Effect of X1 and X2 on Y1

b. Effect of X1 and X2 on Y2 The effect of X1 and X2 on Y2 is shown by Figure

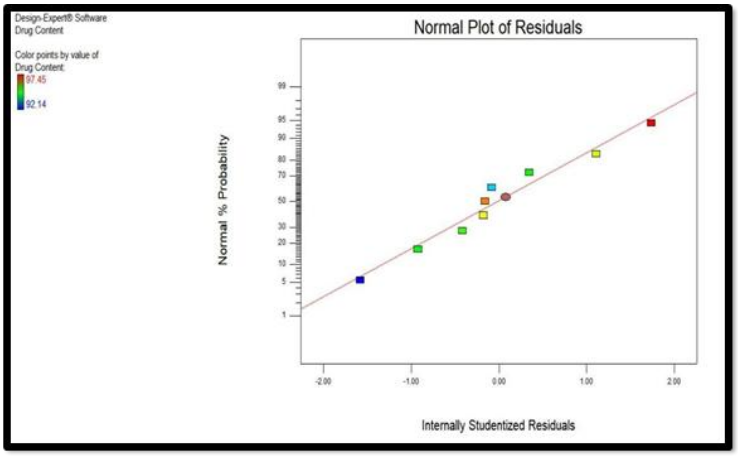

Figure 3Effect of X1 and X2 on Y2

C. Effect of X1 and X2 on Y3

The effect of X1 and X2 on Y3 is shown by Figure

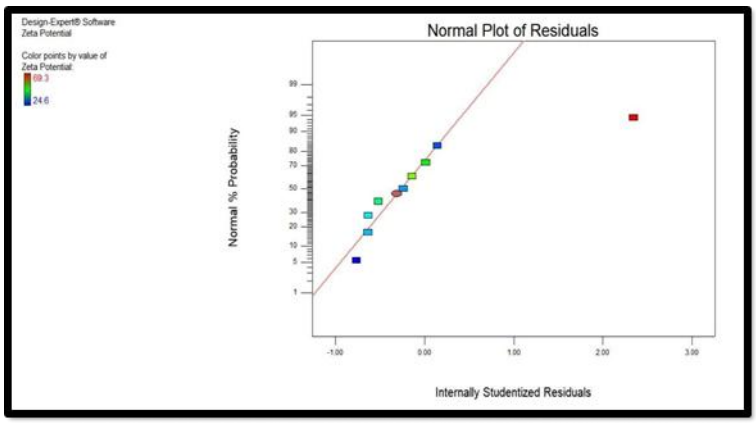

Figure 4Effect of X1 and X2 on Y3

Melting point

Melting point of a drug was determined by open capillary method.

The melting point of telmisartan active pharmaceutical ingredient (API) was determined to confirm the identity and purity of the drug. The study was carried out using a digital melting point apparatus. A small quantity of telmisartan powder was filled into a capillary tube and placed in the apparatus. The sample was heated at a controlled and uniform rate. The temperature at which the drug began to melt and completely melted was carefully observed. Telmisartan exhibited a sharp melting point. The observed melting point was in agreement with reported literature values. This indicated the crystalline nature of the drug. The narrow melting range further confirmed the high purity of telmisartan API.

Preparation of Telmisartan Nanocrystal

Telmisartan nanocrystals were prepared using the antisolvent precipitation technique. An accurately weighed quantity of telmisartan was dissolved in a suitable volume of dichloromethane to form the organic phase. The aqueous antisolvent phase was prepared by dissolving the required amounts of stabilisers, namely PVP K30, PVP K15, or HPMC E15, along with surfactants Poloxamer 188 or Tween 80, in distilled water under continuous stirring. The organic drug solution was then added dropwise into the aqueous phase using a syringe under constant magnetic stirring at a speed of 1200 rpm for 5 hours. The immediate appearance of turbidity indicated the precipitation of telmisartan nanocrystals. The resulting nanosuspension was further stirred to ensure complete solvent diffusion and effective stabilisation of the nanocrystals. The prepared telmisartan nanosuspension was subsequently subjected to further characterisation and evaluation.

Figure 5: Formulations of Nanocrystal (F1-F9)

Characterization and Evaluation of Telmisartan Nanocrystals

The prepared Telmisartan nanocrystals were subjected to comprehensive physicochemical characterization to assess their particle size, stability, solid-state properties and dissolution behaviour.

Particle Size

The mean particle size of the nanosuspension were determined using dynamic light scattering technique with a Malvern Zetasizer. Prior to analysis, the samples were suitably diluted with distilled water to avoid multiple scattering effects. All measurements were carried out at room temperature and the average particle size was recorded in nanometres.

Zeta Potential

The zeta potential of the nanocrystals was measured to evaluate the surface charge and physical stability of the formulation. Higher absolute values of zeta potential indicate greater electrostatic repulsion between particles and better stability of the nanosuspension.

Drug Content

An accurately measured volume of the nanosuspension was diluted with methanol, filtered and analysed using a UV–visible spectrophotometer at the predetermined λmax of Telmisartan. The drug content was calculated using the standard calibration curve.

In-Vitro Drug Release Study

The in-vitro drug release study was carried out using USP Type II (paddle) dissolution apparatus. Phosphate buffer pH 6.8 was used as the dissolution medium, maintained at 37 ± 0.5 °C with a paddle speed of 50 rpm. Samples were withdrawn at predetermined time intervals, filtered and analysed using UV–visible spectrophotometry. The cumulative percentage drug release was calculated.

Scanning Electron Microscopy (SEM)

The surface morphology and shape of the Telmisartan nanocrystals were examined using scanning electron microscopy. Samples were mounted on aluminium stubs, coated with a thin layer of gold and observed at suitable magnifications

Drug Entrapment Efficiency

The drug entrapment efficiency was determined by centrifuging a measured volume of nanosuspension to separate the free drug present in the supernatant. The supernatant was analysed using UV–visible spectrophotometry. High entrapment efficiency indicates effective incorporation of Telmisartan within the nanocrystal formulation.

RESULT AND DISCUSSION

Preformulation studies of Telmisartan

Organoleptic evaluation

The drug was deemed pure since its texture, look, and other attributes met the requirements outlined in the Indian Pharmacopoeia (IP). The IP's description of the drug's sensory qualities also aided in identifying the substance and comprehending its physical characteristics. This demonstrates that the observed characteristics aligned with those of Telmisartan. Table 1 provides a summary of Telmisartan's organoleptic properties.

Table 3 Organoleptic Evaluation of Telmisartan Drug

S. NO.	Sensory characters	Reported (as per IP)	Observed
1	Texture	Powder	Powder
2	Colour	White	White
3	Odour	Odorless	Odorless

Solubility

Telmisartan's solubility was examined in a variety of solvents, such as water, ethanol, Dichloromethane, and methanol. Telmisartan was the most soluble in Dichloromethane all of these. Overall, it was discovered that Telmisartan was insoluble in water but soluble in organic solvents like Dichloromethane alcohol. Table 2 displays Telmisartan's solubility profile.

Table 4 Solubility of Telmisartan Drug in Different Solvent

Drug	**solvent**	**Observation**
Telmisartan	Dichloromethane	+
	Ethanol	+
	Methanol	+
	Water	-

Melting Point

In Indian Pharmacopoeia 2022 the reported melting point of Telmisartan drug was 261-263^0 C. observed Telmisartan drug melting point was around 162^{0}C. Hence it implies with IP standard thus indicating the purity of the sample. The melting point of Telmisartan drug is shown in table 5.

Table 5 Melting Point of Telmisartan Drug

Drugs	**Observed**	**Reference**
Telmisartan	260°C-263°C	261-263° C

Determination of λ_{max} of Telmisartan Drug

Telmisartan wavelength of maximum absorbance (λmax) in Dichloromethane was determined to be 296 nm. Figure 1 displays the Telmisartan calibration curve in dichloromethane. Telmisartan's absorbance and concentration were determined to be linear.

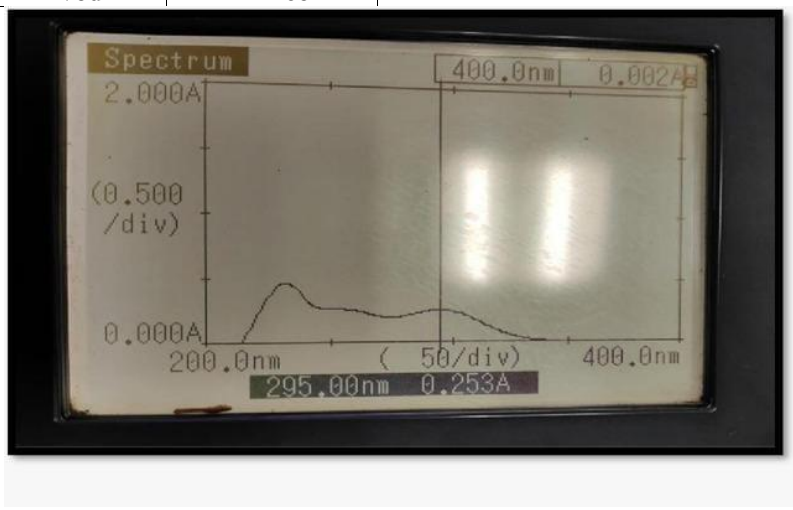

Figure 6Determination of λmax of Telmisartan

Preparation of Standard Calibration Curve in Dichloromethane:

At 296 nm, the absorbances of the standard solutions in methanol in the range of 5-30 µg/mL

were measured. Table 16 and Figure 1 display the standard calibration curve that was created by graphing absorbance (λmax) vs concentration. Regression analysis was used to examine linearity.

Table:

6Calibration Curve of Telmisartan drug

Concentration of Telmisartan Drug (µg/ml)	Absorbance (λ_{max}) at 295nm
5	0.105
10	0.201
15	0.315
20	0.420
25	0.525
30	0.630

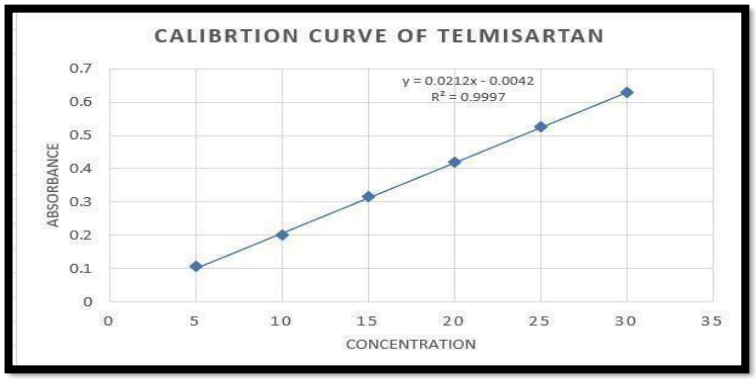

Figure 7Calibration Curve of Telmisartan in Dichloromethane

The linear reversion analysis was done on Absorbance data points. The results are as follow for standard curve Slope = 0.0212 The intercept = 0.0042

The correlation coefficient (r^2) = 0.9997

The calibration curve of Telmisartan was analysed at 295 nm in Dichloromethane

In a UV-visible spectrophotometer. The slope, intercept, and the correlation coefficient were found and the calibration curve was plotted and the correlation coefficient (r^2) was found to be 0.9997.

FTIR of Telmisartan

The FTIR spectrum of pure Telmisartan exhibited characteristic peaks at ~3429 cm^{-1} (N–H/O–H stretching of benzimidazole and carboxylic group), ~3059–3035 cm^{-1} (aromatic C–H stretching), ~2959–2869 cm^{-1} (aliphatic C–H stretching), ~1696 cm^{-1} (C=O stretching of carboxylic acid), ~1599–1520 cm^{-1} (C=C and C=N stretching), ~1267–1229 cm^{-1} (C–O stretching), and ~756–705 cm^{-1} (aromatic C–H bending). These peaks confirmed the structural integrity of Telmisartan.

The FTIR spectra of Telmisartan with PVP K30, Poloxamer 188, and HPMC 615 demonstrated the presence of the same characteristic peaks with minor shifts and broadening in the O–H/N–H (~3429 cm^{-1}) and C=O (~1696 cm^{-1}) regions. Such changes can be attributed to hydrogen bonding and physical interactions between Telmisartan and the polymers. Importantly, no disappearance of characteristic drug peaks was observed, indicating that there is no chemical incompatibility between Telmisartan and the excipients.

This confirms that the selected excipients are compatible with Telmisartan and suitable for the development

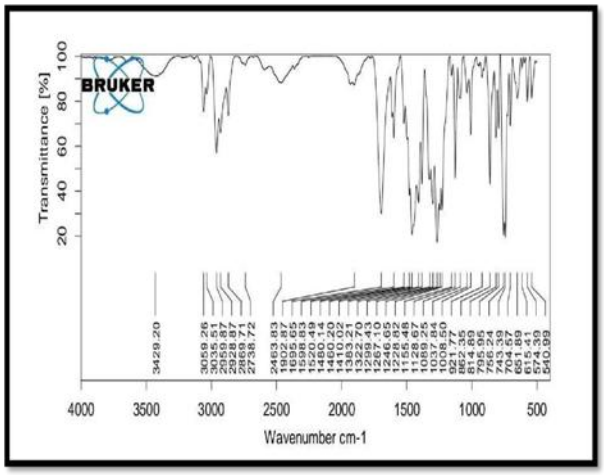

Figure 8FTIR Spectrum of Drug

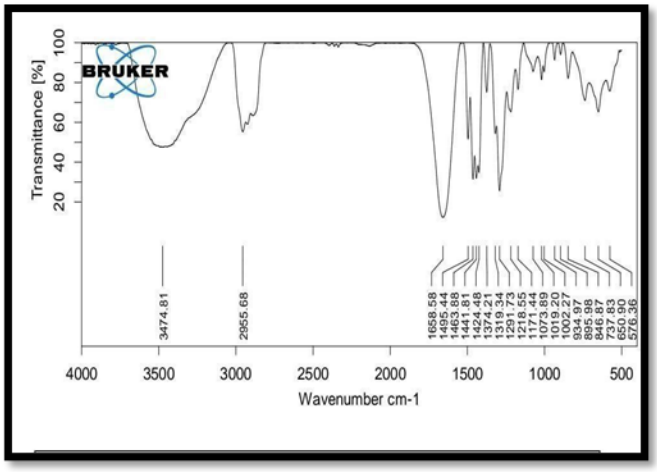

Figure 9 FTIR Spectrum of Drug + PVP K15

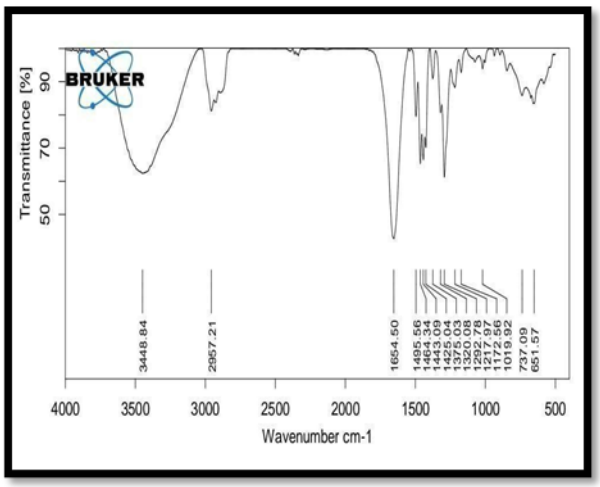

Figure 10FTIR Spectrum of Drug + PVP K30

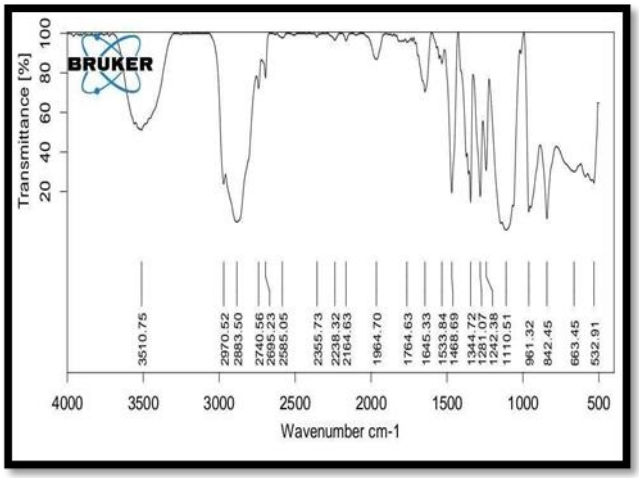

Figure 11FTIR Spectrum of Drug + Poloxamer188

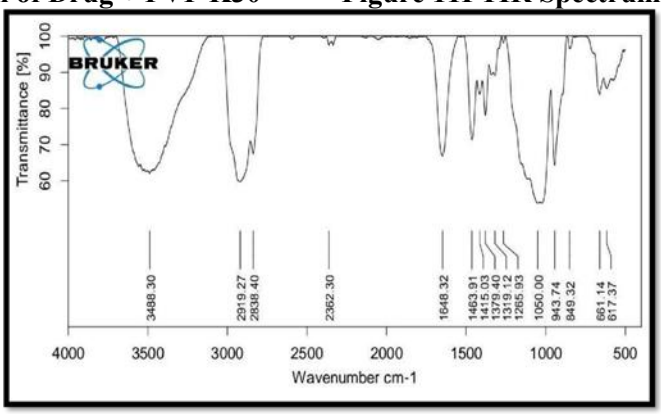

Figure 12FTIR Spectrum of Drug + HPMC E15

Characterization and Evaluation of Particle size Glibenclamide Nanocrystal

Particle size analysis of Telmisartan nanocrystals was carried out using a Nanotrack Wave II particle size analyser at 25–26 °C. The nanosuspensions were diluted with deionised water and sonicated for 1–2 min prior to analysis. Z-average particle size and polydispersity index (PDI) were determined in triplicate and expressed as mean ± SD. PDI was used to evaluate particle size uniformity, with lower values indicating greater homogeneity. Among all formulations, the optimised batch (F7) exhibited the smallest particle size with an acceptable PDI, indicating improved nanosizing efficiency.

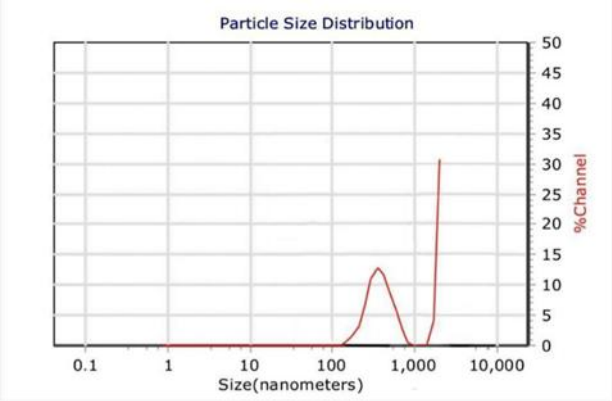

Figure13: Particle Size Distribution of Optimized Telmisartan Nanocrystal Formulation

Zeta potential

Zeta potential of the Telmisartan nanocrystals was determined using electrophoretic light scattering with a Nano ZS (Malvern) instrument. Samples were diluted with deionised water and analysed in disposable zeta cells. Measurements were performed in triplicate and expressed as mean ± SD. The nanocrystals exhibited a high positive zeta potential of +69.3 mV, indicating excellent electrostatic stability and minimal risk of particle aggregation. The strong positive
surface charge, likely due to the presence of cationic stabilizers, contributed to effective electrostatic repulsion, uniform dispersion, and enhanced formulation stability.

Figure14: Zeta Potential of Optimized Telmisartan Nanocrystal Formulation (F7)

Scanning electron microscopy analysis was used to examine the shape and surface Characteristics of coated nanocrystal and porous membrane. At magnification 100 X surface morphology of formulation was examined and it illustrate the smooth surface of nanocrystal. Shape and surface characterization of optimized batch P6 porous membrane and porous coated nanocrystal were shown in figure

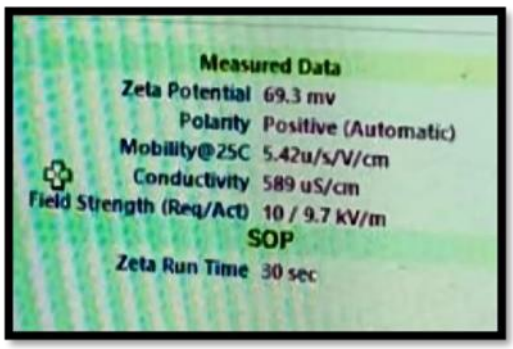

Figure 15: SEM Image Of Optimized Telmisartan Nanocrystal Formulation (F8)

Drug entrapment efficacy

Table 07 summarizes the entrapment efficiency of Telmisartan nanocrystals prepared using formulations F1–F9. A gradual increase in entrapment efficiency was observed with optimization of stabilizer concentration and processing conditions. Among all formulations, F7 showed the highest entrapment efficiency, indicating improved drug loading and stability.

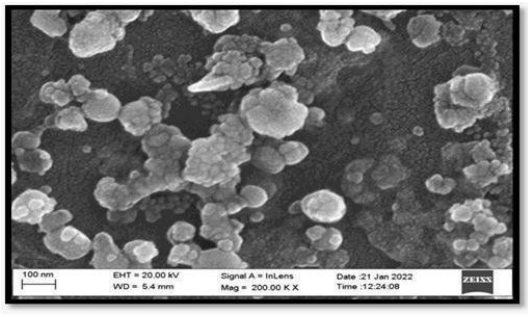

Table 07 Entrapment efficiency of Telmisartan nanocrystals

	Formulation (F1-F9)	Drug Entrapment	Drug content
1	F1	92.85± 0.22	92.14 ± 0.42
2	F2	93.72 ± 0.32	93.25 ± 0.36
3	F3	94.18 ± 0.44	94.86 ± 0.40
4	F4	95.02 ± 0.42	95.12 ± 0.44
5	F5	95.67 ± 0.47	96.04 ± 0.41
6	F6	96.24 ± 0.40	96.78 ± 0.39
7	F7	97.58 ± 0.38	97.45 ± 0.38
8	F8	91.92 ± 0.45	95.89 ± 0.42
9	F9	96.83 ± 0.43	94.73 ± 0.40

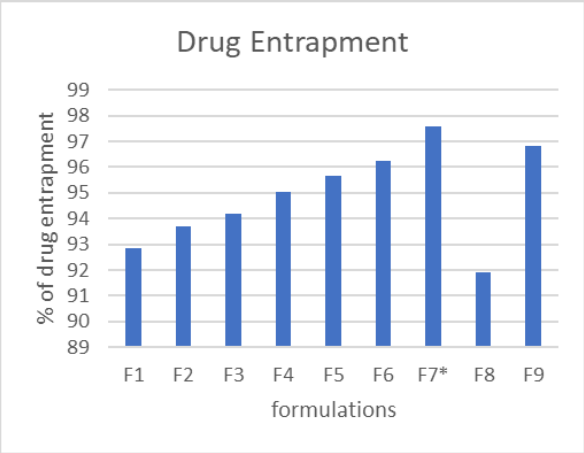

Figure 16Drug entrapment efficiency of telmisartan nanocrystal formulations

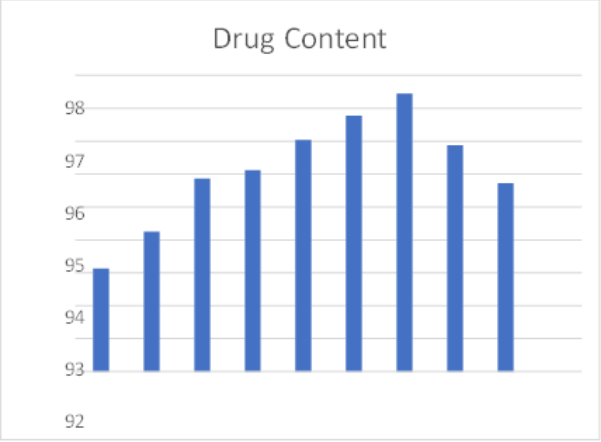

Figure17Comparative drug content of different telmisartan nanocrystal formulations

Drug content

Drug content analysis of Telmisartan nanocrystals (F1–F9) showed values ranging from 92.14 ± 0.42% to 97.45 ± 0.38%, indicating uniform drug loading and good formulation reproducibility. F7 exhibited the highest drug content, attributed to an optimized drug-to-stabilizer ratio, while F1 showed the lowest, highlighting the influence of formulation parameters on drug loading efficiency.

***In-vitro* Drug Release**

The in vitro drug release of Telmisartan nanocrystals was evaluated using a LABINDIA DS 8000 dissolution apparatus (USP Type II, paddle method). Six formulations (F1, F2, F3, F4, F7, and F8) were selected based on particle size, drug content, yield, and stability. Dissolution was performed in 900 mL phosphate buffer (pH 6.8) at 37 ± 0.5 °C and 50 rpm using a dose equivalent to 10 mg of Telmisartan. Samples were withdrawn at predetermined intervals, analyzed by UV–visible spectrophotometry, and cumulative drug release was calculated and plotted against time.

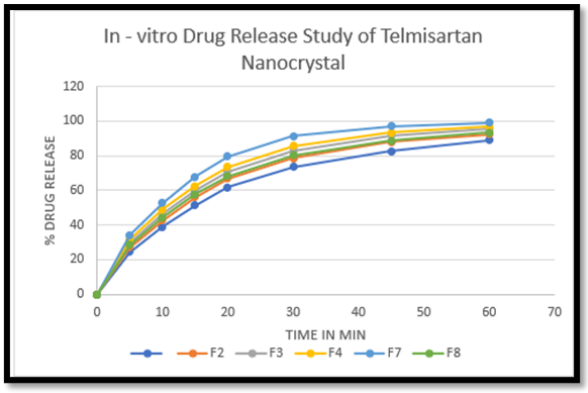

Figure18 In - vitro Drug Release Study of Telmisartan Nanocrystal

The in vitro dissolution data of F7 formulations were fitted to various kinetic models to evaluate the drug release mechanism. Among the studied models, the first-order kinetic model ($R^2 = 0.997$) showed the highest correlation coefficient, indicating that the drug release was primarily concentration-dependent. The Higuchi model ($R^2 = 0.987$) also demonstrated good linearity, suggesting that diffusion played a significant role in the release process. The Korsmeyer–Peppas model ($R^2 = 0.996$) supported the involvement of a combined release mechanism, whereas the zero-order model ($R^2 = 0.915$) showed the lowest correlation. Based on dissolution performance and kinetic evaluation, the F7 batch exhibited the best performance, showing optimal drug release behavior and the highest model fitting, and was therefore considered the optimized formulation

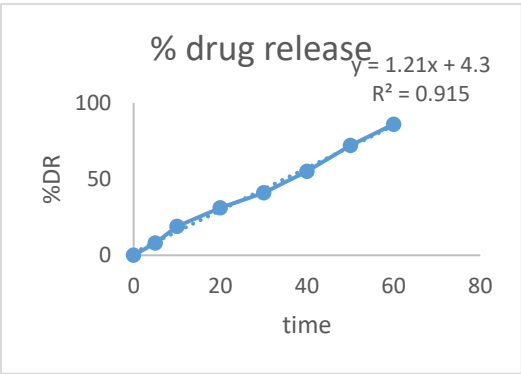

Figure 19 zero order

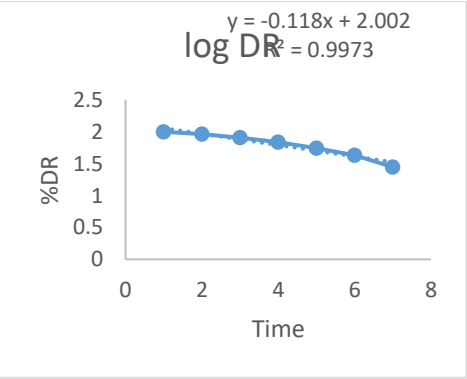

Figure 20 first order

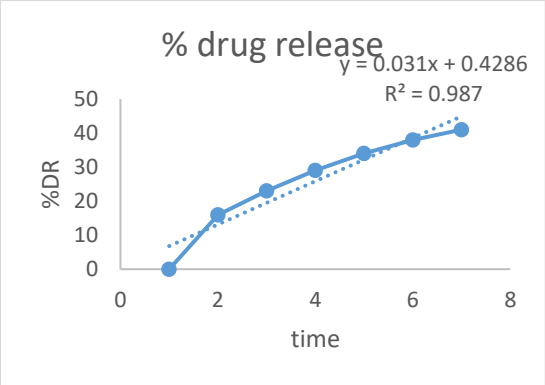

Figure 21 Higuchi model

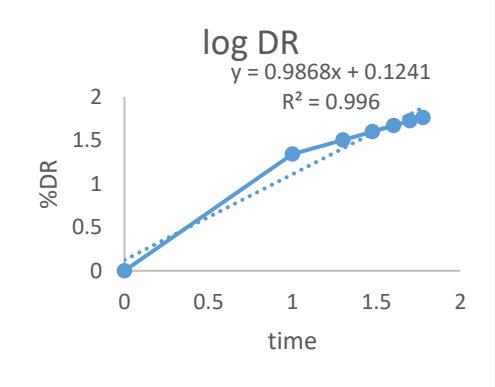

Figure 22 kors -Peppas

The in vitro dissolution data of F1 formulations were analysed using various kinetic models to elucidate the drug release mechanism. Among the evaluated models, the zero-order kinetic model exhibited the highest correlation coefficient (R^2 = 0.9948), indicating a nearly constant drug release rate independent of concentration. The Korsmeyer–Peppas model also showed good linearity (R^2 = 0.9715), suggesting a combined release mechanism involving diffusion and erosion processes. The Higuchi model demonstrated a satisfactory correlation (R^2 = 0.9566), confirming that diffusion contributed significantly to the drug release behaviour. In contrast, the first-order model showed a comparatively lower correlation coefficient (R^2 = 0.9471), indicating that concentration-dependent release was less dominant.

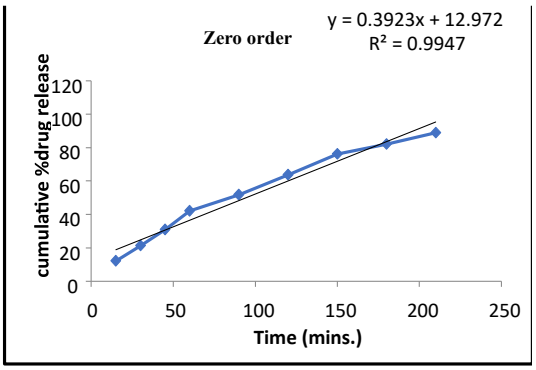

Figure 23 Zero order

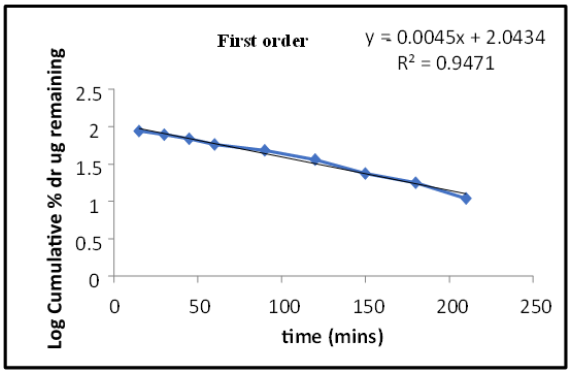

Figure 24 First order

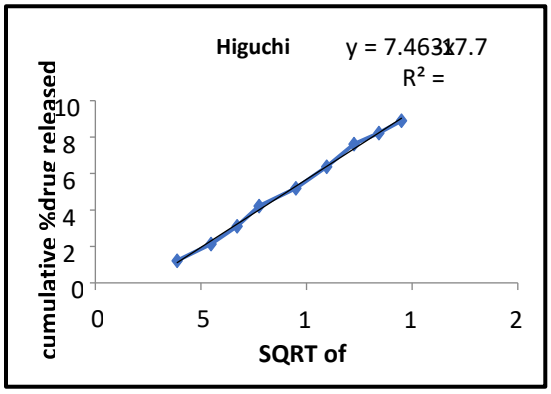

Figure 25 Higuchi

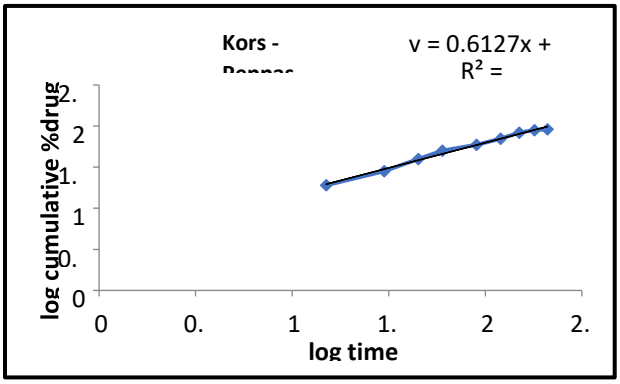

Figure 26 Kors- Peppas

SUMMARY AND CONCLUSION

Conventional oral dosage forms often suffer from limitations such as poor solubility, low bioavailability, frequent dosing, and reduced patient compliance. Novel drug delivery systems, particularly nanocrystals, have gained considerable attention due to their ability to enhance solubility, dissolution rate, and bioavailability of poorly water-soluble drugs like Telmisartan. Nanocrystals offer improved therapeutic efficacy, reduced dosing frequency, and better patient adherence, which are critical for long-term management of hypertension.

In the present study, Telmisartan porous coated nanocrystals were successfully developed and optimized. Preformulation studies confirmed drug compatibility with polymers, as evidenced by FTIR analysis. Nanocrystals were prepared using

the anti-solvent precipitation method and subsequently coated with porous polymer membranes prepared by the solvent evaporation technique. The porous coating enhanced drug loading, stability, and controlled release characteristics.

The formulated nanocrystals were evaluated for morphology, percentage yield, entrapment efficiency, and in vitro drug release. SEM analysis revealed spherical nanocrystals, while the percentage yield ranged from 62.23% to 73.32%, with the highest yield observed for the F7 formulation. In vitro dissolution studies demonstrated improved and controlled drug release from the porous coated nanocrystals.

Among all formulations, F7, prepared using an optimized combination of HPMC, PVP K15, and Tween 80, showed superior entrapment efficiency, controlled drug release, and formulation stability. Thus, porous coated Telmisartan nanocrystals represent a promising and cost-effective delivery system for improving bioavailability, reducing dosing frequency, and enhancing patient compliance in the management of hypertension.

REFERENCES

1. Kesisoglou, F., Panmai, S. and Wu, Y., 2007. Nanosizing—oral formulation development and biopharmaceutical evaluation. *Advanced drug delivery reviews*, *59*(7), pp.631-644.
2. Yameny, A.A., 2024. A Comprehensive Review on Nanoparticles: Definition, Preparation, Characterization, Types, and Medical Applications. *Journal of Medical and Life Science*, *6*(4), pp.663-672.
3. Tiwari D K, Behari J and Sen P 2008 Application of Nanoparticles in Waste Water Treatment 3 417–33.
4. Ealia, S.A.M. and Saravanakumar, M.P., 2017, November. A review on the classification, characterisation, synthesis of nanoparticles and their application. In *IOP conference series: materials science and engineering* (Vol. 263, No. 3, p. 032019).
5. Salavati-niasari M, Davar F and Mir N 2008 Synthesis and characterization of metallic copper

nanoparticles via thermal decomposition Polyhedron 27 3514–8.

6. Tai C Y, Tai C, Chang M and Liu H 2007 Synthesis of Magnesium Hydroxide and Oxide Nanoparticles Using a Spinning Disk Reactor 5536–41.
7. Kumar, S., Naved, T., Alam, S. and Chauhan, R., 2025. Development and Characterization of Telmisartan-Loaded Nanosuspension for Enhanced Drug Delivery. *International Journal of Pharmaceutical Investigation*, *15*(1).
8. Deppe, S., Böger, R.H., Weiss, J. and Benndorf, R.A., 2010. Telmisartan: a review of its pharmacodynamic and pharmacokinetic properties. *Expert opinion on drug metabolism & toxicology*, *6*(7), pp.863-871.
9. Bajaj, A., Rao, M.R., Pardeshi, A. and Sali, D., 2012. Nanocrystallization by evaporative antisolvent technique for solubility and bioavailability enhancement of telmisartan. *AAPS pharmscitech*, *13*(4), pp.1331-1340.
10. Kumar, S., Naved, T., Alam, S. and Chauhan, R., 2025. Development and Characterization of Telmisartan-Loaded Nanosuspension for Enhanced Drug Delivery. *International Journal of Pharmaceutical Investigation*, *15*(1).
11. Junghanns, J.U.A. and Müller, R.H., 2008. Nanocrystal technology, drug delivery and clinical applications. *International journal of nanomedicine*, *3*(3), pp.295-310.
12. Möschwitzer, J.P., 2013. Drug nanocrystals in the commercial pharmaceutical development process. *International journal of pharmaceutics*, *453*(1), pp.142-156.

13. Murr, L.E., 2017. Classifications and structures of nanomaterials. In *Handbook of Materials Structures, Properties, Processing and Performance* (pp. 1-29). Springer, Cham.
14. Barhoum, A., García-Betancourt, M.L., Jeevanandam, J., Hussien, E.A., Mekkawy, S.A., Mostafa, M., Omran, M.M., S. Abdalla, M. and Bechelany, M., 2022. Review on natural, incidental, bioinspired, and engineered nanomaterials: history, definitions, classifications, synthesis, properties, market, toxicities, risks, and regulations. *Nanomaterials*, *12*(2), p.177.
15. Rao, C.N.R., Thomas, P.J. and Kulkarni, G.U., 2007. *Nanocrystals: synthesis, properties and applications*. Berlin, Heidelberg: Springer Berlin Heidelberg.
16. Pardhi, V.P., Verma, T., Flora, S.J.S., Chandasana, H. and Shukla, R., 2018. Nanocrystals: an overview of fabrication, characterization and therapeutic applications in drug delivery. *Current pharmaceutical design*, *24*(43), pp.5129-5146.
17. Rajput, N., 2015. Methods of preparation of nanoparticles-a review. *International Journal of Advances in Engineering & Technology*, *7*(6), p.1806.
18. Stoeva, S.I., Prasad, B.L.V., Uma, S., Stoimenov, P.K., Zaikovski, V., Sorensen, C.M. and Klabunde, K.J., 2003. Face-centered cubic and hexagonal closed-packed nanocrystal superlattices of gold nanoparticles prepared by different methods. *The Journal of Physical Chemistry B*, *107*(30), pp.7441-7448.
19. Jakubek, Z.J., Chen, M., Couillard, M., Leng, T., Liu, L., Zou, S., Baxa, U., Clogston, J.D., Hamad, W.Y. and Johnston, L.J., 2018. Characterization challenges for a cellulose nanocrystal reference material: dispersion and particle size distributions. *Journal of Nanoparticle Research*, *20*(4), p.98.
20. Biswas, A., Bayer, I.S., Biris, A.S., Wang, T., Dervishi, E. and Faupel, F., 2012. Advances in
top–down and bottom–up surface nanofabrication: Techniques, applications & future prospects. *Advances in colloid and interface science*, *170*(1-2), pp.2-27.
21. Schultz, S., Wagner, G., Urban, K. and Ulrich, J., 2004. High-pressure homogenization as a process for emulsion formation. *Chemical Engineering & Technology: Industrial ChemistryPlant Equipment-Process Engineering-Biotechnology*, *27*(4), pp.361-368.
22. Xiong, G., Jiang, X., Xie, F., Fan, Y., Xu, X., Zhang, M., Qi, J., Wang, S. and Zhou, X., 2021. Effect of high-pressure homogenization on structural changes and emulsifying properties of
chicken liver proteins isolated by isoelectric solubilization/precipitation. *LWT*, *151*, p.112092.
23. Stec, M., Synowiec, P.M. and Stolarczyk, A., 2024. Synthesis of HAp by means of sonoprecipitation method. *Materials*, *17*(13), p.3240. Paredes, A.J., Camacho, N.M., Schofs, L., Dib, A., del Pilar Zarazaga, M., Litterio, N., Allemandi, D.A., Bruni, S.S., Lanusse, C. and Palma, S.D., 2020. Ricobendazole nanocrystals obtained by media milling and spray drying: pharmacokinetic comparison with the micronized form of the drug. *International Journal of Pharmaceutics*, *585*, p.119501.
24. Oyinloye, T.M. and Yoon, W.B., 2020. Effect of freeze-drying on quality and grinding process of food produce: A review. *Processes*, *8*(3), p.354.
25. Shegokar, R. and Müller, R.H., 2010. Nanocrystals: industrially feasible multifunctional formulation technology for

poorly soluble actives. *International journal of pharmaceutics*, *399*(1-2), pp.129-139.

26. Thakkar, S., Shah, V., Misra, M. and Kalia, K., 2017. Nanocrystal based drug delivery system: conventional and current scenario. *Recent patents on nanotechnology*, *11*(2), pp.130-145.
27. Macedo, L.D.O., Masiero, J.F. and Bou-Chacra, N.A., 2024. Drug nanocrystals in oral absorption: factors that influence pharmacokinetics. *Pharmaceutics*, *16*(9), p.1141.
28. Gigliobianco MR, Casadidio C, Censi R, Di Martino P. Nanocrystals of Poorly Soluble Drugs: Drug Bioavailability and Physicochemical Stability. *Pharmaceutics*. 2018;10(3):134. Published 2018 Aug 21.
29. Lhaglham, P., Jiramonai, L., Jia, Y., Huang, B., Huang, Y., Gao, X., Zhang, J., Liang, X.J. and Zhu, M., 2024. Drug nanocrystals: Surface engineering and its applications in targeted delivery. *Iscience*, *27*(11).
30. Grim, J.Q., Manna, L. and Moreels, I., 2015. A sustainable future for photonic colloidal nanocrystals. *Chemical Society Reviews*, *44*(16), pp.5897-5914.
31. Kovalenko, M.V., Manna, L., Cabot, A., Hens, Z., Talapin, D.V., Kagan, C.R., Klimov, V.I., Rogach, A.L., Reiss, P., Milliron, D.J. and Guyot-Sionnnest, P., 2015. Prospects of nanoscience with nanocrystals. *ACS nano*, *9*(2), pp.1012-1057.
32. Yang, W., Jo, S.H. and Lee, T.W., 2024. Perovskite colloidal nanocrystal solar cells: current advances, challenges, and future perspectives. Advanced Materials, *36*(29), p.2401788.
33. Müller, R. H., Gohla, S., & Keck, C. M. (2011). State of the art of nanocrystals – Special features, production, nanotoxicology issues and intracellular delivery. European Journal of Pharmaceutics and Biopharmaceutics, 78(1), 1–9.
34. Keck, C. M., & Müller, R. H. (2006). Drug nanocrystals of poorly soluble drugs produced by high pressure homogenization. European Journal of Pharmaceutics and Biopharmaceutics, 62(1), 3–16.
35. Kakran, M., Sahoo, N. G., Li, L., & Judeh, Z. (2012). Fabrication of quercetin nanocrystals y anti-solvent precipitation method for enhanced dissolution. *Powder Technology*, 223, 59–64.
36. Borghese, C., Casarsa, C., & Pivetta, T. (2022). Rational formulation strategies to improve redispersion of drug nanocrystals after freeze-drying. International Journal of Pharmaceutics, 623, 121932.
37. Bilati, U., Allémann, E., & Doelker, E. (2005). Nanocrystal formation in freeze-dried polymerbased nanosuspensions. Drug Development and Industrial Pharmacy, 31(3), 231–243.
38. Chen, J., Ouyang, D., Xu, H., & Zhong, Y. (2019). Nanocrystal-loaded fast dissolving oral films for improved bioavailability of poorly soluble drugs. *International Journal of Pharmaceutics*, 569, 118593.
39. Lu, Y., Chen, S., Wang, Z., & Liu, S. (2016). Mucoadhesive polymer-coated nanocrystals for enhanced intestinal absorption of hydrophobic drugs. *Acta Pharmaceutica Sinica B*, 6(6), 582– 589.

HOW TO CITE: Dr. Nimita Manocha, Garima Bairagi, Nayany Sharma, Dr. Nadeem Farooqui, Telmisartan - nanocrystal innovative approach to enhance oral bioavailability, Int. J. of Pharm. Sci., 2026, Vol 4, Issue 5, 4503-4518, https://doi.org/10.5281/zenodo.20268436